






ORIGINAL ARTICLE OPEN ACCESS

pSTAT3 Expression is Increased in Advanced Prostate Cancer in Post-Initiation of Androgen Deprivation Therapy

Piotr Bialas^{1,2}  | Tamae Kobayashi¹ | Rebecka Hellsten¹  | Agnieszka Krzyzanowska¹  | Margareta Persson³ | Felicia Marginean¹ | Dominique Trudel^{4,5} | Isla P. Garraway^{6,7} | Bruce J. Trock⁸ | Pekka Taimen^{9,10} | Fred Saad¹¹ | Tuomas Mirtti^{12,13}  | Beatrice Knudsen¹⁴ | Angelo M. De Marzo^{8,15,16} | Anders Bjartell^{1,17} 

¹Department of Translational Medicine, Division of Urological Cancers, Lund University, Malmö, Sweden | ²Chair and Department of Cell Biology, Poznan University of Medical Sciences, Poznan, Poland | ³Department of Laboratory Medicine, Translational Cancer Research, Lund University, Lund, Sweden | ⁴Centre de recherche du Centre hospitalier de l'Université de Montréal et Institut du cancer de Montréal, Montreal, Quebec, Canada | ⁵Department of Pathology and Cellular Biology, Université de Montréal, Montreal, Quebec, Canada | ⁶Department of Urology, Jonsson Comprehensive Cancer Center, David Geffen School of Medicine at University of California, Los Angeles, California, USA | ⁷Division of Urology, Greater Los Angeles VA Healthcare System, Los Angeles, California, USA | ⁸Department of Urology and Brady Urological Institute, Johns Hopkins University School of Medicine, Baltimore, Maryland, USA | ⁹Institute of Biomedicine and FICAN West Cancer Centre, University of Turku, Turku, Finland | ¹⁰Department of Pathology, Turku University Hospital, Turku, Finland | ¹¹Department of Surgery, Université de Montréal, Montreal, Quebec, Canada | ¹²HUS Diagnostic Center, Department of Pathology, HUS Helsinki University Hospital, Helsinki, Finland | ¹³Medicum and Research Program In Systems Oncology, Faculty of Medicine, University of Helsinki, Helsinki, Finland | ¹⁴Digital and Computational Pathology, University of Utah, Salt Lake City, Utah, USA | ¹⁵Department of Pathology, Johns Hopkins University School of Medicine, Baltimore, Maryland, USA | ¹⁶Department of Oncology and The Sidney Kimmel Comprehensive Cancer Center at Johns Hopkins, Baltimore, Maryland, USA | ¹⁷Department of Urology, Skåne University Hospital, Malmö, Sweden

Correspondence: Anders Bjartell (anders.bjartell@med.lu.se)

Received: 5 August 2024 | **Revised:** 14 October 2024 | **Accepted:** 23 October 2024

Funding: This work was supported by Swedish Scientific Council, ALF Lund University, Kungliga Fysiografiska Sällskapet i Lund, Movember Foundation, NIH/NCI SPORE, Fonds de Recherche du Québec-Santé and Swedish Cancer Foundation.

Keywords: androgen deprivation therapy | androgens | biomarkers | prostate cancer | STAT3

ABSTRACT

Background: The transcription factor Signal Transducer and Activator of Transcription 3 (STAT3) plays a role in carcinogenesis and is involved in processes, such as proliferation, differentiation, drug resistance and immunosuppression. STAT3 can be activated by phosphorylation of tyrosine at position 705 (pSTAT3^{Tyr705}) or serine at 727 (pSTAT3^{Ser727}). High expression levels of pSTAT3 are implicated in advanced stages of prostate cancer (PCa) and are known to interact with the androgen receptor signaling pathway. However, not much is known about how androgen deprivation therapy (ADT) in advanced disease affects pSTAT3 expression. The aim of this study was to determine the influence of ADT on pSTAT3 expression in PCa tissue.

Methods: The study cohort came from a PCa tissue microarray resource containing prostate specimens from patients before and post-initiation of ADT. Tissue samples from 111 patients were immunostained for pSTAT3^{Tyr705} and pSTAT3^{Ser727}. H-score was used to evaluate the intensity and the percentage of pSTAT3 expression in malignant epithelial and stromal compartments. Univariate and multivariable Cox regression analyses were used to assess pSTAT3^{Tyr705} and pSTAT3^{Ser727} as biomarkers of oncological outcome in patients undergoing ADT.

Abbreviations: ADT, androgen deprivation therapy; AR, androgen receptor; CAF, cancer-associated fibroblasts; CRPC, castration-resistant prostate cancer; EGF, epidermal growth factor; FGF, fibroblast growth factors; GAP1, Movember Global Action Plan 1; MFS, metastasis-free survival; OS, overall survival; PCa, prostate cancer; STAT3, signal transducer and activator of transcription; TMA, tissue microarray; TURP, transurethral resection of the prostate; VEGF, vascular endothelial growth factor.

This is an open access article under the terms of the [Creative Commons Attribution-NonCommercial-NoDerivs](https://creativecommons.org/licenses/by-nc-nd/4.0/) License, which permits use and distribution in any medium, provided the original work is properly cited, the use is non-commercial and no modifications or adaptations are made.

© 2024 The Author(s). *The Prostate* published by Wiley Periodicals LLC.

Results: Post-ADT PCa samples demonstrated increased nuclear and cytoplasmic levels of pSTAT3^{Ser727} in the stroma compared to pre-ADT samples, whereas pSTAT3^{Tyr705} expression was increased significantly in both stromal and malignant epithelial compartments except for stromal cytoplasm. High cytoplasmic pSTAT3^{Ser727} in stromal compartments correlated with reduced overall survival, shorter time to castration-resistant PCa development, and decreased metastasis-free survival. An increase in nuclear and cytoplasmic pSTAT3^{Ser727} expression within the stromal compartment of post-ADT samples corresponded to a shorter time to CRPC development, which was not observed for pSTAT3^{Tyr705}. Multivariable survival analysis using Cox's regression identified that high cytoplasmic pSTAT3^{Ser727} expression in the stroma of post-ADT samples and pT3 or pT4-stage were associated with worse overall survival and 5-year metastasis-free survival (MFS).

Conclusions: This study presents novel insights into the impact of ADT on the expression levels of pSTAT3^{Tyr705} and pSTAT3^{Ser727} in PCa. Cytoplasmic pSTAT3^{Ser727} status of cancer-associated stromal cells in post-ADT samples may serve as an independent prognostic marker for OS and 5-year MFS, identifying prostate cancer patients prone to developing resistance to ADT.

1 | Introduction

Prostate cancer (PCa) is the most prevalent nonskin malignancy in Western countries. In 2020, the World Health Organization reported approximately 1.4 million new cases worldwide, with about 0.46 million men succumbing to the disease [1]. The risk factors contributing to PCa development include age, ethnicity and genetic predispositions including mutations in the *BRCA1/2* and *HoxB13* [2]. Despite significant advancements in early detection and treatments, with improved overall survival (OS), around 10%–20% of men with localized disease develop metastasis [3]. New and more useful biomarkers and prediction models are needed to better stratify patients with various aggressiveness to select the most appropriate treatment regimens.

Treatment of patients with advanced PCa involves targeting androgen signaling since the prostate relies on androgens for biological functioning. Androgen deprivation therapy (ADT) means surgical or pharmacological castration, depending on the specific characteristics of the individual patient [4]. Unfortunately, almost every patient on ADT will over time develop castration-resistant prostate cancer (CRPC). Hence, there is a need to understand the mechanisms driving treatment resistance and identify predictive and prognostic biomarkers and novel therapeutic targets for CRPC, allowing for adjustments and personalized treatment plans dedicated to unique patient characteristics. Modern treatment of CRPC should aim at combination therapies targeting multiple pathways simultaneously by combining androgen receptor (AR)-targeted therapies with poly (ADP-ribose) polymerase (PARP) inhibitors, immunotherapy and other novel agents to enhance treatment efficacy [4].

Several studies have highlighted the importance of the transcription factor Signal Transducer and Activator of Transcription 3 (STAT3) in tumorigenesis. The STAT3 signaling pathway is implicated in carcinogenesis and involves processes like proliferation, differentiation, survival, metastatic spread, angiogenesis, drug resistance and immunosuppression [5–7]. STAT3 function is tightly regulated and can be activated through the phosphorylation of tyrosine 705 (pSTAT3^{Tyr705}) or serine 727 (pSTAT3^{Ser727}) and it depends on binding cytokines (IL-6, IL-10, and IL-11) or growth factors (EGF, FGF, VEGF) to cell surface receptors which activate the tyrosine phosphorylation cascade in the canonical pathway [8]. STAT3 may also regulate the expression of immunosuppressive markers and activate immunosuppressive

cells to create a tumor microenvironment promoting cancer cell survival [9]. In PCa, STAT3 has shown to be involved in cancer progression, from the early stages to the advanced metastatic castration-resistant state and has emerged as a therapeutic target with ongoing research to develop STAT3 inhibitors [10]. We have previously described a lower nuclear expression of pSTAT3^{Tyr705} and pSTAT3^{Ser727} in both epithelium and stromal tissues within cancerous areas compared to noncancerous regions in PCa tissue obtained from hormone-naïve localized PCa patients undergoing radical prostatectomy. The lower expression of both pSTAT3 forms demonstrated a correlation with a shorter period leading to biochemical recurrence (BCR) [11]. Furthermore, it has been suggested that differential expression of pSTAT3 could play a role in developing metastatic lesions [12]. Increased levels of pSTAT3^{Tyr705} were noted within the bone compared to lymph nodes and visceral metastatic sites, indicating that tissue microenvironment may influence pSTAT3^{Tyr705} expression [13]. There is a need to understand better the interplay between malignant cells and the surrounding tumor stroma. In this study, we investigated the pSTAT3 expression in malignant epithelium and the corresponding stromal compartments in advanced PCa patients before (pre-ADT) and during androgen deprivation therapy (post-ADT).

2 | Materials and Methods

2.1 | Patient Cohort and Sample Collection

The study material consisted of a unique PCa tissue microarray (TMA) from Movember Global Action Plan 1 (GAP1) [14]. The collection included tissue materials from each participating hospital's pathology department, where patients underwent medical procedures such as biopsy, surgery, or transurethral resection of the prostate (TURP) between 1978 and 2016. Multiple institutes and hospitals participated in GAP1 including the Johns Hopkins Hospital, the Helsinki University Central Hospital, the Turku University Hospital, the Cedars-Sinai Medical Center and the University of Washington. All institutions involved received ethical review board permission to use patient material and conduct the study. A total of 114 patients were enrolled in the Movember GAP1 project; however, samples from three individuals were missing in sections from the TMA construct. In pSTAT3^{Ser727} staining, samples from 111 patients were available; however, in the case of pSTAT3^{Tyr705}

10 patients were excluded from analysis due to the unsatisfactory quality of tissue cores (Figure 1).

In this study, PCa tissue samples from patients collected prior (pre-ADT) and after commencing ADT (post-ADT) that is, orchiectomy or gonadotropin-releasing hormone agonists/antagonists, were used. The first-line treatment included various approaches: ADT was administered to 75 patients, 10 patients received a combination of ADT and radiotherapy, 13 underwent radical prostatectomy, 7 received radiotherapy, and 6 individuals were subjected to another type of treatment. The initial treatment had a median duration of 48.5 months, ranging from 1.2 to 227 months, while the period from initiation of ADT to collection of samples had a median duration of 46.2 months (0.6–233); (Table 1). Matched tissue samples from the same individuals collected before and after initiation of ADT were accessible for analysis in a subset of patients.

2.2 | Immunohistochemistry

Formalin-fixed paraffin-embedded (FFPE) tissue specimens from PCa patients were used for TMA construction according to standard operating procedures. Briefly, a minimum of three cores from prostatic tissue or metastatic lesions (when accessible); (0.6 or 1 mm) were transferred to a final TMA block in a serial manner. As internal controls for staining quality, xenografts of PCa human cell lines were used. TMA slides were

deparaffinized with xylene and ethanol followed by rehydration and antigen retrieval. The antigen retrieval step was performed using a PT-Link module (DAKO, Glostrup, Denmark) at 95°C–99°C for 20 min (pH 9.0). The slides were then stained in a DAKO Autostainer-plus using the EnVision FLEX, including Peroxidase-Blocking Reagent (DAKO). Subsequently, TMAs were immunostained for pSTAT3^{Ser727} (CS9134, 1:100; Cell Signaling Technology, Danvers, MA) or pSTAT3^{Tyr705} (ab76315, 1:100; Abcam, Cambridge, UK). The selected commercially available antibodies for this study were chosen based on earlier uses [11] after conducting thorough laboratory validation using test sample collections.

2.3 | Scoring of Tissue Microarrays

Tissue microarrays were scanned using an Aperio CS2 slide scanner, and the images obtained were viewed on the Aperio ImageScope Software (Leica Biosystems, Wetzlar, Germany). The samples underwent revision by a pathologist (coauthor F.M.) to determine the benign areas, and only cores comprising at least 90% cancerous regions were included for analysis in the present study. The intensity of the cytoplasmic and nuclear staining in the malignant epithelial cells and accompanying stroma was manually marked as a score in the range from 0 up to 3 (no expression, low, moderate, and high; respectively) and the percentage of nuclei and cytoplasm-stained area was also evaluated (< 5% = 0.5, 5%–33% = 1, 34%–66% = 2, > 66% = 3).

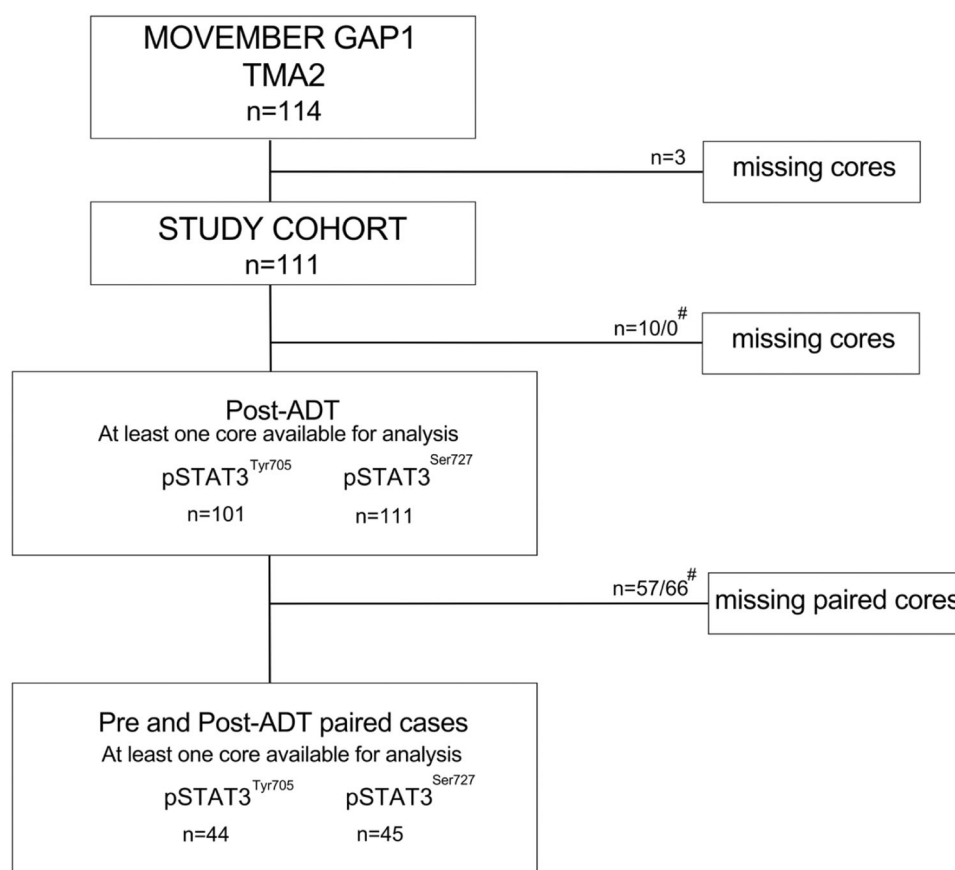


FIGURE 1 | Consort diagram of patients included in the study. # indicates absent cores in the case of pSTAT3^{Tyr705} and pSTAT3^{Ser727}, respectively.

TABLE 1 | Patient characteristics.

	All (n = 111)	Pre-and post-ADT only (n = 45)
Age at diagnosis (years)	67 (median) range: 49–85	67 (median) range: 49–85
< 50	1 (1%)	1 (2.2%)
50–59	26 (23.4%)	11 (24.4%)
60–69	37 (33.3%)	15 (33.4%)
> 70	47 (42.3%)	18 (40.0%)
Diagnosis method		
Biopsy	75 (67.6%)	29 (64.4%)
TURP	18 (16.2%)	8 (17.8%)
Unknown	18 (16.2%)	8 (17.8%)
Type of post-ADT specimen		
Biopsy	1 (0.9%)	1 (2.2%)
TURP	92 (82.9%)	28 (62.3%)
Prostatectomy	2 (1.8%)	2 (4.4%)
Metastasis	16 (14.4%)	14 (31.1%)
Clinical stage		
T1	16 (14.4%)	4 (8.9%)
T2	25 (22.5%)	5 (11.1%)
T3	10 (9.0%)	4 (8.9%)
T4	10 (9.0%)	2 (4.4%)
Unknown	50 (45.1%)	30 (66.7%)
Surgical margins		
Positive	5 (4.5%)	5 (13.3%)
Negative	6 (5.4%)	6 (11.1%)
Unknown	100 (90.1%)	34 (75.6%)
PSA at the time of diagnosis (ng/ml)		
Median	28.7	24.0
Mean	68.2	64.4
Range	2.2–540	3.9–540
Pre-ADT specimen gleason sum		
≤ 6	11 (10%)	2 (4.4%)
7	27 (24.3%)	11(24.4%)
8	16 (14.4%)	5 (11%)
9	18 (16%)	10 (22.2%)
10	2 (2%)	1 (2%)
Missing	37 (33.3%)	16 (36%)
Extraprostatic extension		
Positive	9 (8.1%)	9 (20%)
Negative	2 (1.8%)	2 (4.4%)
Unknown	100 (90.1%)	34 (75.6%)
Seminal vesicle invasion		
Positive	5 (4.5%)	5 (11%)

TABLE 1 | (Continued)

	All (n = 111)	Pre-and post-ADT only (n = 45)
Negative	6 (5.4%)	5 (11%)
Unknown	100 (90.1%)	35 (78%)
Lymph node involvement		
Positive	2 (1.8%)	2 (4%)
Negative	9 (8.1%)	8 (18%)
Unknown	100 (90.1%)	35 (78%)

The intensity score and the fraction of positively stained cells were multiplied to receive a final score result (h-score on a scale: 0–9, adapted from Detre et al. [15]) and then h-scores were used to represent the expression level in each given patient. Immunostained blood vessels identified within the tissue cores were omitted from the final score. The scoring was assessed by two independent investigators (co-authors: P.B. and M.P.). A consensus between the investigators on how to evaluate immunostainings was reached before the scoring. The results were based on the average score of no less than three patients' cores, but in the rare cases of missing cores, the score of one or two cores was used instead.

2.4 | Statistical Analysis

All the statistical analyses were conducted using IBM SPSS Statistics v. 25 (Armonk, NY, USA) and Statistica software v. 14.0.1.25 (StatSoft, Uppsala, Sweden). The Shapiro-Wilk test was used to assess data normality. Mean intensity scores were compared using both the paired t-test and the Wilcoxon matched pairs test for group comparisons. To evaluate correlations between two groups, Spearman's Rank Correlation Coefficient (Rs) was utilized [16], and moderate and strong correlation was defined as above 0.5 or above 0.7, respectively. Kaplan-Meier estimator was used to plot the survival curves. The cutoffs used in the Kaplan-Meier estimator that categorized the patients into low and high expression were based on the median value. Log-rank test or Cox's F-Test were used to determine the p-value in observations: the interval from diagnosis to the last follow-up (overall survival; OS), the interval from primary treatment to CRPC development, and the interval from primary treatment to the occurrence of metastasis (metastasis-free survival; MFS). Univariate and multivariable proportional hazard regression analyses were performed to determine the predictive values of the different markers. *p* values ≤ 0.05 were considered as significant.

3 | Results

3.1 | pSTAT3 Expression in Tissue Microarray Samples

Immunohistochemical analysis revealed distinct subcellular patterns for pSTAT3^{Tyr705} and pSTAT3^{Ser727}. pSTAT3^{Tyr705} was

predominantly located in the nucleus, while pSTAT3^{Ser727} demonstrated a more heterogeneous distribution, being detected in both the nuclear and cytoplasmic compartments. Figure 2 shows examples of nuclear and cytoplasmic expression of pSTAT3^{Tyr705} and pSTAT3^{Ser727} in malignant epithelial or stromal tissue of pre- and post-ADT paired cases that came from needle biopsy (pre-ADT) and TURP (post-ADT) obtained from the same patient.

The expression levels of pSTAT3^{Tyr705} and pSTAT3^{Ser727} in the malignant epithelial tissue and stromal compartments in pre- and post-ADT tissue samples were quantified using the h-score methodology (Figure 3, Supporting Information S1: Figure S1). In malignant epithelial cells, pSTAT3^{Tyr705} expression was significantly increased in both nuclei and cytoplasm in patients following ADT compared to matched samples taken at pre-ADT (Figure 3A). pSTAT3^{Ser727} was increased in the epithelial tissue post-ADT, but not statistically significant (Figure 3C). In the stroma, pSTAT3^{Ser727} expression was significantly increased in both nuclei and cytoplasm in post-ADT samples compared to pre-ADT (Figure 3D). pSTAT3^{Tyr705} was significantly higher in stromal nuclei but not in the cytoplasm of post-ADT samples compared to pre-ADT (Figure 3B). Waterfall charts were used to visualize the observed alterations in the h-scores of pSTAT3^{Tyr705} and pSTAT3^{Ser727}, comparing post-ADT to pre-ADT samples (Supporting Information S1: Figure S2).

The Spearman's rank correlation tests were implemented to assess potential correlations among the h-scores within studied subcellular compartments in pre- and post-ADT samples (Supporting Information S1: Table S1). The analysis demonstrated a weak positive correlation between the h-scores of pSTAT3^{Tyr705} in the malignant epithelial nuclear expression before and after ADT ($rs = 0.425$, $p < 0.01$). Conversely, the

pSTAT3^{Ser727} expression within the same tissue types consistently presented a strong positive correlation between nuclear and cytoplasmic compartments, both in the pre-ADT group (malignant epithelium, $rs = 0.697$, $p > 0.01$; stroma, $rs = 0.696$, $p > 0.01$) and the post-ADT groups (malignant epithelium, $rs = 0.708$, $p > 0.01$; stroma, 0.636 , $p > 0.01$); (Supporting Information S1: Table S1). A correlation in h-scores for pSTAT3^{Tyr705} between subcellular expressions was observed in malignant epithelium in post-ADT samples ($rs = 0.533$, $p > 0.01$); (Supporting Information S1: Table S1). Additionally, a positive correlation was found between malignant epithelial and stromal cytoplasmic pSTAT3^{Tyr705} in post-ADT samples ($rs = 0.583$, $p < 0.01$); (Supporting Information S1: Table S1). Further analyses unveiled a positive correlation between changes in the delta h-score of pSTAT3^{Tyr727} due to ADT in the nuclei and cytoplasm, both in the malignant epithelium ($rs = 0.628$, $p > 0.01$) and stroma ($rs = 0.728$, $p > 0.01$); (Supporting Information S1: Table S2).

3.2 | Outcome Analysis

Patient stratification based on high or low expression levels of pSTAT3^{Ser727} and pSTAT3^{Tyr705} in post-ADT samples was illustrated using Kaplan–Meier survival analyses for outcomes in terms of patient OS, time to develop CRPC and metastases-free survival (MFS); (Figure 4, Supporting Information S1: Figure S3). With regard to the stromal compartment, survival analyses demonstrated that patients with high cytoplasmic pSTAT3^{Ser727} expression among those who underwent ADT had decreased OS ($p = 0.013$; Figure 4B), decreased MFS ($p = 0.034$; Figure 4D) and shorter time to develop CRPC ($p = 0.042$; Figure 4H). Moreover, we noticed a significantly shorter time to CRPC among the patients that presented high nuclear

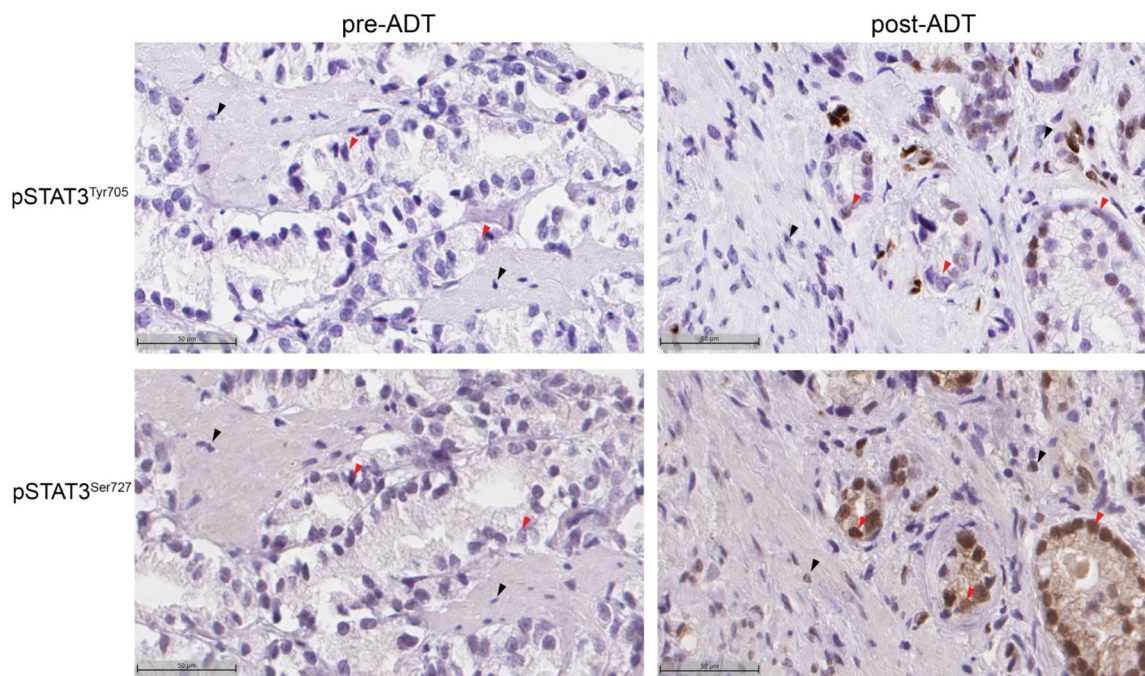


FIGURE 2 | Representative images of pSTAT3^{Tyr705} (A, B) and pSTAT3^{Ser727} (C, D) immunostainings. Pre-ADT and post-ADT examples for each staining are from the same patient. Scale bar = 50 μ m. The arrowhead indicates examples of the epithelium (red) and stroma (black). [Color figure can be viewed at [wileyonlinelibrary.com](https://onlinelibrary.wiley.com)]

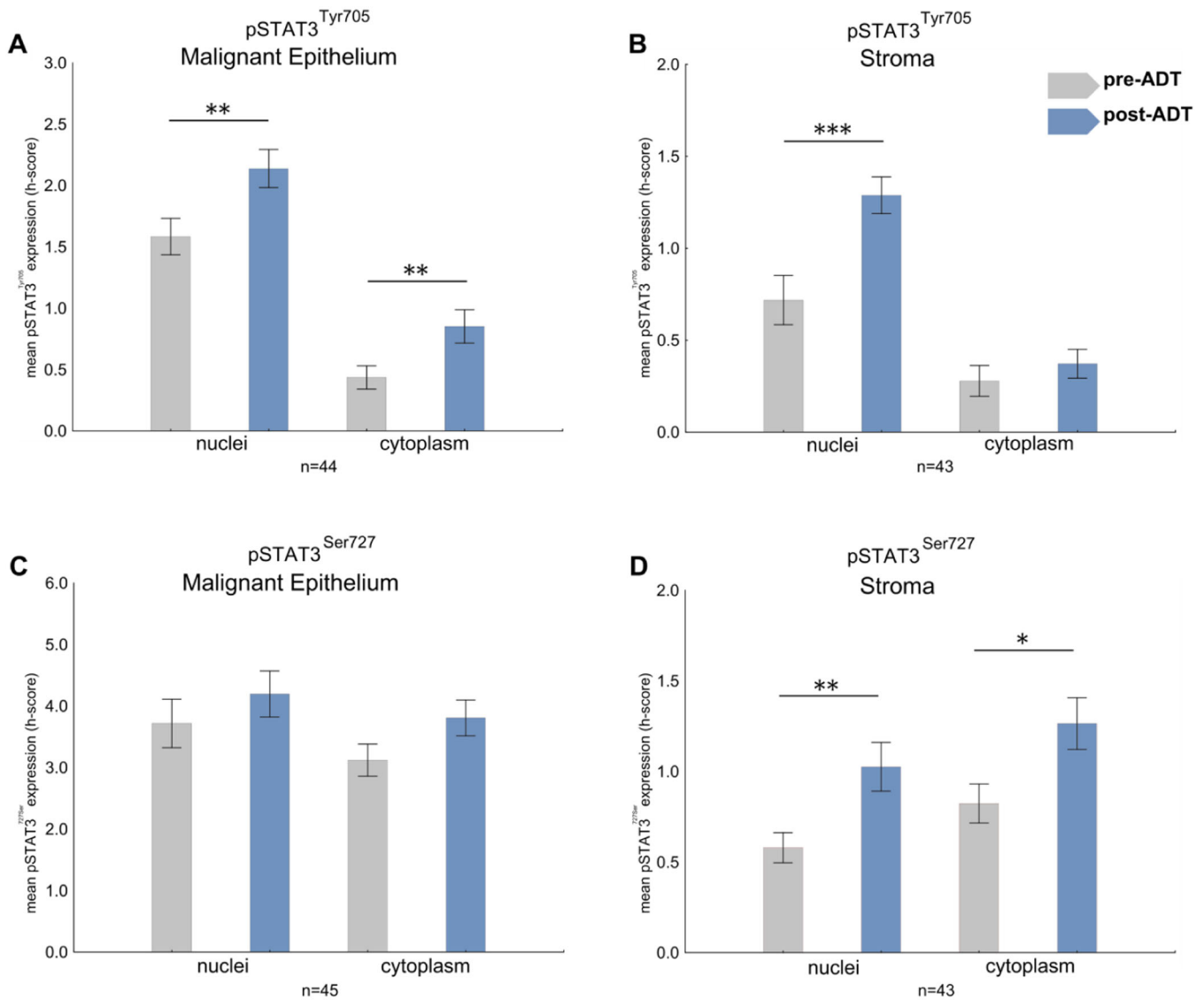


FIGURE 3 | Nuclear and cytoplasmic expression of pSTAT3^{Tyr705} (A, B) and pSTAT3^{Ser727} (C, D) in the stroma or epithelium of pre-ADT and post-ADT paired tissue samples. Expression presented as average h-score. Wilcoxon signed-rank and paired *t*-test statistic test were used to calculate *p* value. *p* ≤ 0.05 was considered significant. **p* ≤ 0.05, ***p* ≤ 0.01, ****p* ≤ 0.001. Data presented as mean ± SEM. [Color figure can be viewed at [wileyonlinelibrary.com](https://onlinelibrary.wiley.com)]

expression of pSTAT3^{Ser727} in stromal cells (*p* = 0.015; Figure 4F). We did not observe any significant differences when analyzing the corresponding cellular compartments for pSTAT3^{Tyr705} expression in stromal cells (Figure 4A,C,E,G). With regard to the epithelial compartment, high cytoplasmic pSTAT3^{Tyr705} expression in carcinoma cells in post-ADT tissue samples was associated with a longer time to CRPC (*p* = 0.01, Supporting Information S1: Figure S3B). However, we did not observe a similar association in the case of nuclear pSTAT3^{Tyr705} expression (*p* = 0.41, Supporting Information S1: Figure S3A). Neither cytoplasmic nor nuclear pSTAT3^{Ser727} expression of carcinoma cells was associated with time to CRPC (Supporting Information S1: Figure S3C,D).

We also categorized patients into two subgroups according to the changes in pSTAT3 expression before and during ADT in matched samples: one group presented an increase in pSTAT3 expression levels, and the other group demonstrated a decrease

or no change in pSTAT3 expression (Figure 5). Our analysis revealed differences between analyzed subgroups associated with time to CRPC development. Patients with an increased expression of pSTAT3^{Ser727} in both the nuclear and cytoplasmic compartments of stromal cells demonstrated a significantly shorter time to CRPC (*p* = 0.043 and *p* = 0.018, respectively) (Figure 5B,D). No difference in time to CRPC was observed for pSTAT3^{Tyr705} expression changes (Figure 5A,C). Furthermore, our analysis revealed no significant differences in the time to CRPC development based on the change of either nuclear or cytoplasmic pSTAT3^{Tyr705} expression of carcinoma cells (Figure 5E,F).

Using univariate COX proportional hazard regression analysis, we examined associations between distinct factors and clinical outcomes (Table 2). In the post-ADT patient group cytoplasmic expression of pSTAT3^{Ser727} within stromal compartments and the pT-stage were significantly associated with OS (HR = 1.79,

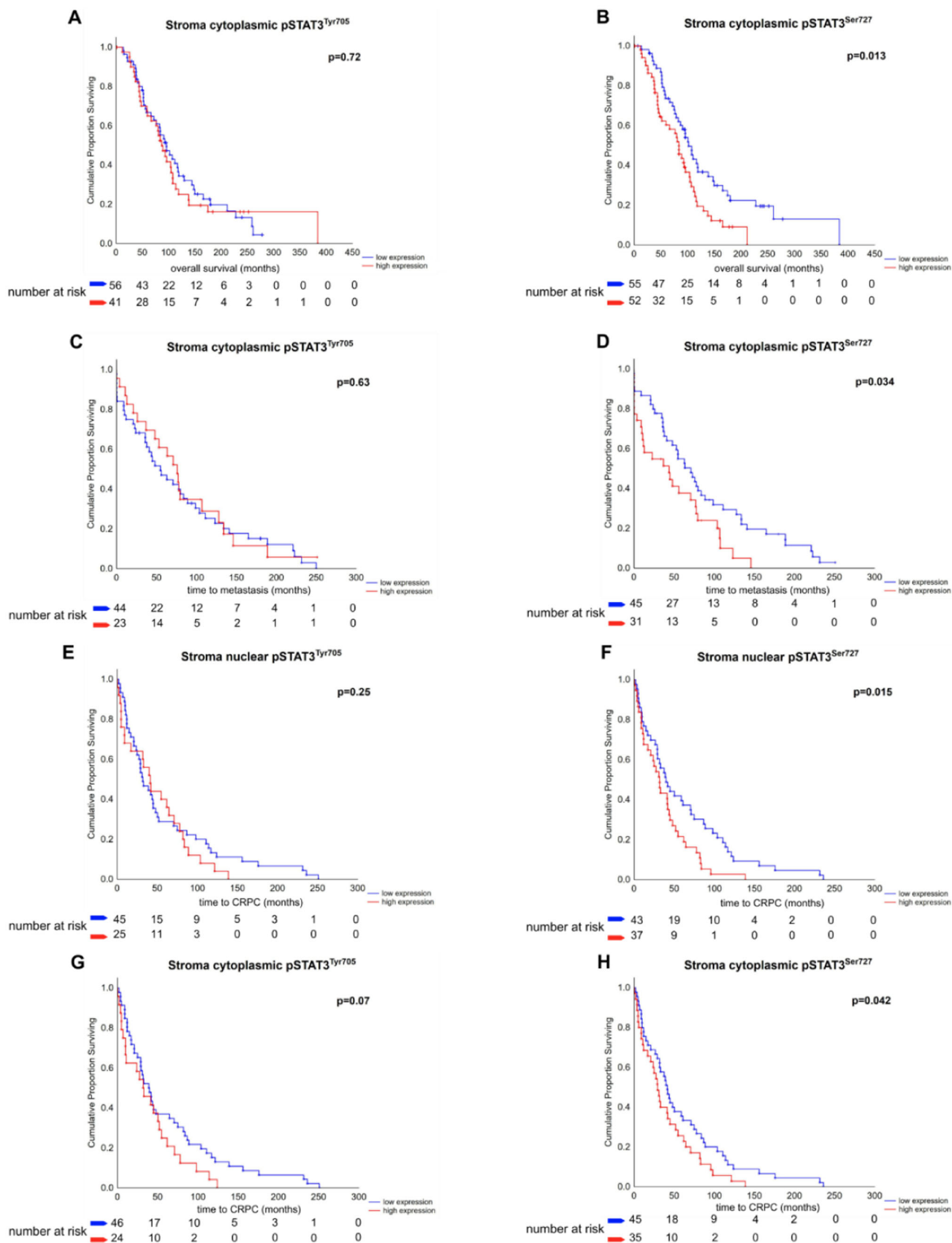


FIGURE 4 | Kaplan-Meier curves of OS (A, B), time to metastasis (C, D), and time to CRPC (E–H) for expression of pSTAT3^{Tyr705} and pSTAT3^{Ser727} in post-ADT tissue samples. Cox’s *F*-test and Log-rank statistic tests were used to calculate *p* value. $p \leq 0.05$ was considered significant. [Color figure can be viewed at [wileyonlinelibrary.com](https://onlinelibrary.wiley.com)]

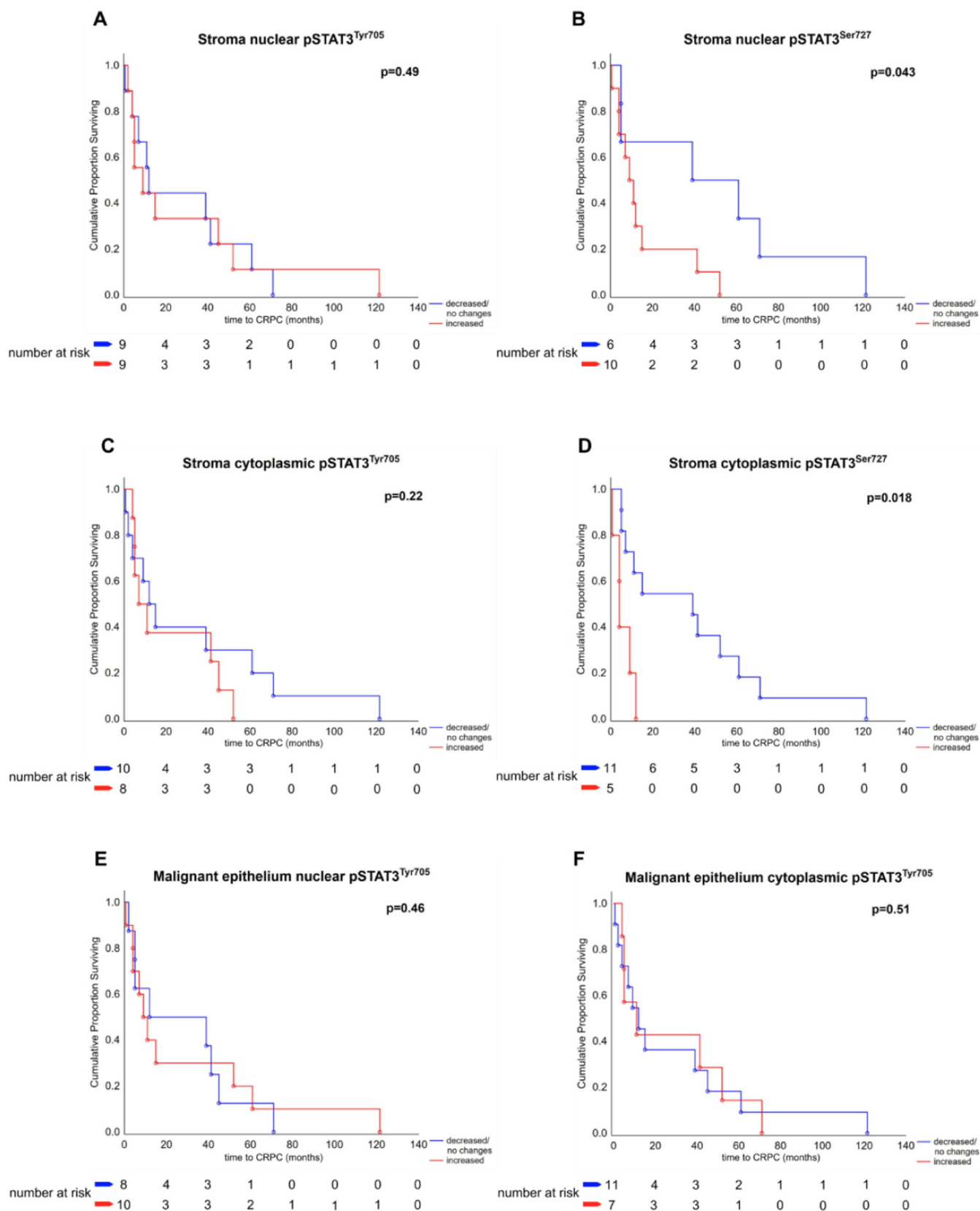


FIGURE 5 | Kaplan-Meier curves of time to CRPC development in expression changes from pre-ADT to post-ADT of (A) pSTAT3^{Tyr705} and (B) pSTAT3^{Ser727} in stromal nuclei, expression of (C) pSTAT3^{Tyr705} and (D) pSTAT3^{Ser727} in stromal cytoplasm, (E) pSTAT3^{Tyr705} in malignant epithelial nuclei and (F) pSTAT3^{Tyr705} in malignant epithelial cytoplasm. Cox's *F*-test was used to calculate the p-value. $p \leq 0.05$ was considered significant. [Color figure can be viewed at [wileyonlinelibrary.com](https://onlinelibrary.wiley.com)]

TABLE 2 | Cox univariable and multivariable regression analysis for pSTAT3^{Ser727} expression: in stroma cytoplasm post-ADT in the interval from diagnosis to last follow-up (A), in the interval from primary treatment to 5 years of survival without metastasis (B), in the interval from primary treatment to 3-years of survival without castrate-resistant prostate cancer (CRPC); (C). $p \leq 0.05$ was considered significant.

	Univariable			Multivariable		
	HR	95% CI	<i>p</i>	HR	95% CI	<i>p</i>
A. Observation: time from diagnosis to last follow up						
pSTAT3 ^{Ser727} expression in stroma cytoplasm post-ADT (low = ref.) high	1.79	1.15–2.8	0.01	1.94	1.23–3.07	0.004
PSA (< 10 ng/mL = ref.) > 10 ng/ml	1.06	0.49–2.25	0.89	0.85	0.4–1.81	0.67
Gleason score (< 7 = ref.) ≥ 7	1.51	0.87–2.61	0.14	1.52	0.88–2.62	0.13
T stage (T1–T2 = ref.) T3–T4	2.08	1.13–3.83	0.02	2.19	1.14–4.20	0.02
B. Observation: time from primary treatment to 5-years of survival without metastasis						
pSTAT3 ^{Ser727} expression in stroma cytoplasm post-ADT (low = ref.) high	1.76	0.95–3.27	0.07	2.11	1.10–4.02	0.02
PSA (< 10 ng/mL = ref.) > 10 ng/ml	0.73	0.29–1.83	0.5	0.52	0.18–1.49	0.23
Gleason score (< 7 = ref.) ≥ 7	2.15	1.00–4.59	0.05	1.94	0.88–4.28	0.10
T stage (T1–T2 = ref.) T3–T4	2.27	1.08–4.76	0.03	2.40	1.09–5.25	0.03
C. Observation: time from primary treatment to 3-years of survival without castrate-resistant prostate cancer						
pSTAT3 ^{Ser727} expression in stroma cytoplasm post-ADT (low = ref.) high	1.26	0.63–2.53	0.51	1.26	0.63–2.51	0.52
PSA (< 10 ng/ml = ref.) > 10 ng/ml	0.82	0.18–3.72	0.79	0.54	0.12–2.52	0.43
Gleason score (< 7 = ref.) ≥ 7	1.96	0.8–4.84	0.14	2.25	0.91–5.57	0.08
T stage (T1–T2 = ref.) T3–T4	1.93	0.58–6.48	0.29	2.6	0.70–9.67	0.16
pSTAT3 ^{Ser727} expression in stroma nuclei post-ADT (low = ref.) high	1.95	0.97–3.92	0.06	1.90	0.94–3.84	0.07
PSA (< 10 ng/mL = ref.) > 10 ng/ml	0.82	0.18–3.72	0.79	0.61	0.13–2.89	0.53
Gleason score (< 7 = ref.) ≥ 7	1.96	0.8–4.84	0.14	2.08	0.86–5.04	0.10
T stage (T1–T2 = ref.) T3–T4	1.93	0.58–6.48	0.29	2.69	0.74–9.77	0.13
pSTAT3 ^{Tyr705} expression in epithelial cytoplasm post-ADT (low = ref.) high	0.87	0.56–1.34	0.52	0.96	0.58–1.59	0.88
PSA (< 10 ng/mL = ref.) > 10 ng/ml	0.82	0.18–3.72	0.79	0.56	0.11–2.71	0.47
Gleason score (< 7 = ref.) ≥ 7	1.96	0.8–4.84	0.14	2.24	0.88–5.69	0.09
T stage (T1–T2 = ref.) T3–T4	1.93	0.58–6.48	0.29	2.51	0.64–9.84	0.19

CI: 1.15–2.8; $p = 0.01$, and HR = 2.08, CI: 1.13–3.83; $p = 0.02$, respectively). Moreover, Gleason score and pT-stage were also significantly associated with 5-year MFS (HR = 2.15, CI: 1.00–4.59; $p = 0.05$, and HR = 2.27, CI: 1.08–4.76; $p = 0.03$, respectively). Multivariable COX proportional hazard regression analysis demonstrated that pSTAT3^{Ser727} cytoplasmic expression in stromal compartments and pT-stage in the group of patients following ADT were independent prognostic factors and were significantly associated with OS (HR = 1.94, CI: 1.23–3.07; $p = 0.004$, and HR = 2.19, CI: 1.14–4.20; $p = 0.02$, respectively) and 5-year MFS (HR = 2.11, $p = 0.02$, and HR = 2.4, $p = 0.03$, respectively). On the other hand, univariate and multivariable proportional hazard regression analysis did not present any significant association in pSTAT3 expression with time to 3-year CRPC free survival (Table 2).

4 | Discussion

Expression of active STAT3 in the phosphorylated forms pSTAT3^{Ser727} and pSTAT3^{Tyr705} has previously been demonstrated in PCa tissue [11, 13, 17, 18] and the STAT3 signaling pathway has shown to play a role in the development and progression of PCa [19, 20]. Moreover, studies have described that there is an interplay between STAT3 and AR [21–24], which is considered a fundamental factor in PCa biology.

In this study, we analyzed the nuclear and cytoplasmic expression of pSTAT3^{Ser727} and pSTAT3^{Tyr705} in both the malignant epithelium and the stromal compartment of PCa samples to investigate the potential impact of ADT on their expression levels and determine whether there is an association with outcomes. We observed an increased expression of nuclear and cytoplasmic pSTAT3^{Tyr705} and pSTAT3^{Ser727} in PCa tissues in patients undergoing ADT compared to samples taken before treatment initiation. The primary goal of ADT is to reduce the transmission of AR signaling pathways [25]. PCa cells can independently of androgens develop alternative mechanisms to proliferate, migrate, and survive [26]. Modulation of the activity and expression of the AR via the IL-6/JAK/STAT3 pathway has been documented in metastatic CRPC patients with a decreased response to the second-generation AR inhibitor enzalutamide [27]. The levels of circulating IL-6 are observed to be increased in CRPC and are implicated in resistance to ADT [28–30]. IL-6 may enhance the transcriptional activity of AR both in an androgen dependent and independent manner mediated via JAK/STAT3 and MAPK signaling pathways [23, 31]. There is a direct interaction between STAT3 and the N-terminal domain of AR induced by IL-6 leading to regulation of the transcriptional activity of AR [23]. Thus, STAT3 may play an important role via AR even under ADT. Inhibition of AR signaling with enzalutamide is shown to increase pSTAT3^{Ser727} but not in pSTAT3^{Tyr705} in LNCaP cells and STAT3 inhibition enhanced the sensitivity of PCa cells to enzalutamide [32, 33]. Conversely, the overexpression of constitutively active STAT3 led to the development of resistance against enzalutamide treatment [34]. Our current findings provided additional clinical evidence that high stromal expression of pSTAT3^{Ser727} in post-ADT is an independent prognostic marker for 5-y MFS, suggesting a role of STAT3 activation in stromal cells under ADT for treatment resistance and metastasis progression. Further analysis of

STAT3 activation related to AR expression or their targeted gene expression analysis in stromal cells will be needed to understand the role of STAT3 in stromal cells for tumor progression. Hence, the crosstalk between the AR and IL6/JAK/STAT3 needs to be explored in the framework of developing novel therapies in advanced PCa.

The functional role of STAT3 within the stromal compartment may be distinct from its role within the malignant epithelial tissue. Specifically, within the stromal compartment, STAT3 assumes a role in the induction and function of cancer-associated fibroblasts (CAF) and immune cells, thereby contributing to the establishment of an immunosuppressive and tumor-supportive microenvironment [35]. STAT3 is involved in signaling pathways regulating the activity of cytokines and growth factors [36]. CAFs may promote tumor growth by secreting IL-6 and VEGF, both subject to STAT3-mediated regulation [37]. The action of STAT3 within the stromal context extends beyond PCa, as evidenced by the presence of analogous observations in diverse malignancies, including breast cancer oral squamous cell carcinoma [38, 39]. In contrast to our earlier findings, where low stromal STAT3^{Ser727} expression in hormone-naïve prostate cancer patients' tissue samples was associated with worse clinical outcomes [17], the current study showed higher stromal STAT3^{Ser727} expression after ADT was associated with poor clinical outcome. These findings suggest the different roles of STAT3^{Ser727} in modulating immune activities in TME before and after ADT. CAF is one of the major components of stromal cell types in TME that can also mediate STAT3 activities to impact on the TME [40–42]. Reprogramming of stromal cells and CRPC promotion by ADT and CAF have also been reported [43]. Since this process involves ERK and TGF β signaling, it will be intriguing to investigate in the future whether pSTAT3^{Ser727} activation also has a role in such TME reprogramming and influence on CRPC progression under ADT. Furthermore, the evaluation of the pSTAT3 expression in stromal cells associated with immune cell infiltration and immune suppression needs to be explored in future studies.

In addition, the involvement of pSTAT3^{Ser727} in mitochondrial respiration has been established through its regulatory influence on electron transfer chain complex activities and transcriptional processes, thereby modulating mitochondrial metabolism [44]. In the present study, high expression of STAT3^{Ser727} in stromal cytoplasm was associated with shorter OS, 5-year MFS, and time to CRPC development within a cohort of patients subjected to ADT. Furthermore, our study pointed out that the expression of STAT3^{Ser727} within the stromal cytoplasmic compartment may serve as an independent prognostic biomarker for OS and MFS in patients undergoing ADT.

The prognostic role of pSTAT3^{Ser727} has been demonstrated in other malignancies. In a study of clear cell renal cell carcinoma, pSTAT3^{Ser727} was described as an independent prognostic factor for OS [45]. Detailed analyses indicated that patients diagnosed with advanced stage of clear cell renal cell carcinoma which demonstrated high pSTAT3^{Ser727} expression in either the nucleus or cytosol were associated with a poor prognosis regarding OS.

We observed that high levels of cytoplasmic pSTAT3^{Ser727} expression in the stromal compartment post-ADT were associated with worse clinical outcomes. Comparable observations were

published by Morrow et al. where the study demonstrated that a reduction in the 5-year survival rate among patients diagnosed with triple-negative breast cancer was closely linked to expression levels of total STAT3 in the stromal compartment [46]. However, this study did not differentiate between the phosphorylated forms of STAT3.

There are certain limitations to our study. First, our cohort consisted of a limited number of samples, particularly in the context of stratifying patients into distinct groups based on increased and decreased/no changes in expression for cumulative proportion survival analyses. This limitation arose from the absence of full clinical data for the studied patients and missing cores, especially within the group before the administration of ADT. Consequently, we were unable to perform a comprehensive pre-post analysis for the entire cohort. Secondly, the heterogeneity of pre-ADT treatments should also be considered as a limitation. Additionally, some patients received multiple rounds of ADT, while the duration of drug treatment varied from mere months to several years. Intra-tumoral heterogeneity is another concern in TMA studies. It is worth noting that, despite these limitations, our observations appear to be valuable and need to be repeated within a larger patient cohort.

5 | Conclusions

This study documented novel insights on the impact of ADT on the expression levels of pSTAT3^{Tyr705} and pSTAT3^{Ser727} in PCA tissue. The study highlights that the presence of pSTAT3^{Ser727} in the stromal cytoplasm may serve as a biomarker for predicting the OS and MFS in individuals subjected to ADT. Furthermore, high pSTAT3^{Ser727} expression in the stromal cytoplasm of PCA lesions is linked to unfavorable clinical outcome, like reduced OS and shorter time to development of metastasis.

Author Contributions

The authors confirm their contribution to the manuscript as follows: study conception and design: Piotr Bialas, Rebecka Hellsten, Agnieszka Krzyzanowska, Anders Bjartell. Data collection: Dominique Trudel, Bruce J. Trock, Fred Saad, Tuomas Mirtti, Angelo M. De Marzo. Organized and assisted in scoring the immunohistochemical stains: Margareta Persson, Piotr Bialas, Agnieszka Krzyzanowska, Tamae Kobayashi. Quality control and pathology review of supplied TMA analysis: Felicia Marginean. Interpretation of results: Agnieszka Krzyzanowska, Piotr Bialas, Rebecka Hellsten, Tamae Kobayashi, Anders Bjartell. Statistical analysis: Piotr Bialas, Agnieszka Krzyzanowska, Tamae Kobayashi. Writing review of draft and editing: Piotr Bialas, Tamae Kobayashi, Rebecka Hellsten, Anders Bjartell. All authors reviewed the results and approved the final version of the manuscript.

Acknowledgments

We are grateful to Kristina Ekström-Holka and Emelie Karnevi for technical assistance in the staining, scanning, and organizing processes. We thank the following principal investigators for providing tissue material and data; Kathy Wiley, Colm Morrissey, Viktor Berge, Carlos S. Moreno, Kristin Austlid Tasken, Lawrence D. True, Michael S. Lewis, Aud Svindland, Onur Ertunc, Igor Damasceno Vidal, Adeboye O. Osunkoya, Tracy Jones, G. Steven Bova, Tarja Lamminen, Steven A. Bigler, Xinchun Zhou, Stephen J. Freedland, Anne-Marie Mes-Masson. We also thank the rapid Autopsy Team, Celestia Higano, Pete Nelson,

Bruce Montgomery, Evan Yu, Elahe Mostaghel, Paul Lange, Robert Vessella, Xiaotun Zhang, and Martine Roudier for contributing to the rapid autopsy programs and Gayle Walters for legal support. This work was supported by grants from the Swedish Cancer Society (Cancerfonden, 21 1629 Pj 01 H), and the Swedish Scientific Council (Vetenskapsrådet, 2020-02017), ALF (Lund University), the Skåne University Hospital Research Foundations, Kungliga Fysiografiska Sällskapet i Lund (43193). B.J. Trock, P. Taimen, F. Saad, T. Mirtti, B.S. Knudsen, and A.M. De Marzo were funded by Movember. B.J. Trock and A.M. De Marzo from JHU were supported by U.S. NIH/NCI SPORE in Prostate Cancer: P50CA58236, the U.S. Department of Defense Prostate Cancer Research Program (PCRP): W81XWH-18-2-0015 to A.M. De Marzo. Johns Hopkins Sidney Kimmel Comprehensive Cancer Center Oncology Tissue Services Laboratory supported by U.S. NIH/NCI P30 CA006973 (to B.J. Trock and A.M. De Marzo). CRCHUM was supported by the FRQS (to F. Saad and D. Trudel) and their Biobanking at the CRCHUM was done in collaboration with the Réseau de recherche sur le cancer supported by the Fonds de Recherche Québec - Santé (FRQ-S) affiliated to the Canadian Tissue Repository Network (CTRNet). F. Saad holds the Raymond Garneau Chair in Prostate Cancer. D. Trudel was supported by the Chercheure boursière clinique niveau junior 2 of the FRQ-S awards.

Ethics Statement

All involved institutions received ethical review board permission to use patient material which was conducted in accordance with ethical guidelines.

Conflicts of Interest

AB and RH are cofounders and shareholders in Glactone Pharma AB.

Data Availability Statement

The data that support the findings of this study are available from the corresponding author upon reasonable request.

References

1. L. Wang, B. Lu, M. He, Y. Wang, Z. Wang, and L. Du, "Prostate Cancer Incidence and Mortality: Global Status and Temporal Trends in 89 Countries From 2000 to 2019," *Frontiers in Public Health* 10 (2022): 811044, <https://doi.org/10.3389/FPUBH.2022.811044>.
2. G. Attard, C. Parker, R. A. Eeles, et al., "Prostate Cancer," *Lancet* 387, no. 10013 (2016): 70–82, [https://doi.org/10.1016/S0140-6736\(14\)61947-4](https://doi.org/10.1016/S0140-6736(14)61947-4).
3. N. N. Nafissi, H. E. Kosiosek, R. J. Butterfield, et al., "Evolving Natural History of Metastatic Prostate Cancer," *Cureus* 12, no. 11 (2020): 11484, <https://doi.org/10.7759/CUREUS.11484>.
4. C. Dai, S. M. Dehm, and N. Sharifi, "Targeting the Androgen Signaling Axis in Prostate Cancer," *Journal of Clinical Oncology* 41, no. 26 (2023): 4267–4278, <https://doi.org/10.1200/JCO.23.00433>.
5. X. Wang, P. J. Crowe, D. Goldstein, and J. L. Yang, "STAT3 Inhibition, a Novel Approach to Enhancing Targeted Therapy in Human Cancers," *International Journal of Oncology* 41, no. 4 (2012): 1181–1191, <https://doi.org/10.3892/IJO.2012.1568>.
6. H. Yu, H. Lee, A. Herrmann, R. Buettner, and R. Jove, "Revisiting STAT3 Signalling in Cancer: New and Unexpected Biological Functions," *Nature Reviews Cancer* 14, no. 11 (2014): 736–746, <https://doi.org/10.1038/NRC3818>.
7. I. Tošić and D. A. Frank, "STAT3 as a Mediator of Oncogenic Cellular Metabolism: Pathogenic and Therapeutic Implications," *Neoplasia* 23, no. 12 (2021): 1167–1178, <https://doi.org/10.1016/J.NEO.2021.10.003>.
8. M. El-Tanani, A. O. Al Khatib, S. M. Aladwan, A. Abuelhana, P. A. McCarron, and M. M. Tambuwala, "Importance of STAT3 Signalling

- in Cancer, Metastasis and Therapeutic Interventions,” *Cellular Signalling* 92 (2022): 110275, <https://doi.org/10.1016/J.CELLSIG.2022.110275>.
9. Y. Dong, J. Chen, Y. Chen, and S. Liu, “Targeting the STAT3 Oncogenic Pathway: Cancer Immunotherapy and Drug Repurposing,” *Biomedicine & Pharmacotherapy = Biomedecine & Pharmacotherapie* 167 (2023): 115513, <https://doi.org/10.1016/J.BIOPHA.2023.115513>.
10. H. Lee, A. J. Jeong, and S. K. Ye, “Highlighted STAT3 as a Potential Drug Target for Cancer Therapy,” *BMB Reports* 52, no. 7 (2019): 415–423, <https://doi.org/10.5483/BMBREP.2019.52.7.152>.
11. A. Krzyzanowska, N. Don-Doncow, F. E. Marginean, et al., “Expression of tSTAT3, pSTAT3727, and pSTAT3 705 in the Epithelial Cells of Hormone-Naïve Prostate Cancer,” *The Prostate* 79, no. 7 (2019): 784–797, <https://doi.org/10.1002/PROS.23787>.
12. M. Tolomeo and A. Cascio, “The Multifaced Role of STAT3 in Cancer and Its Implication for Anticancer Therapy,” *International Journal of Molecular Sciences* 22, no. 2 (2021): 603, <https://doi.org/10.3390/IJMS22020603>.
13. N. Don-Doncow, F. Marginean, I. Coleman, et al., “Expression of STAT3 in Prostate Cancer Metastases,” *European Urology* 71, no. 3 (2017): 313–316, <https://doi.org/10.1016/J.EURURO.2016.06.018>.
14. V. Ouellet, A. Erickson, K. Wiley, et al., “The Movember Global Action Plan 1 (GAP1): Unique Prostate Cancer Tissue Microarray Resource,” *Cancer Epidemiology, Biomarkers & Prevention* 31, no. 4 (2022): 715–727, <https://doi.org/10.1158/1055-9965.EPI-21-0600>.
15. S. Detre, G. Saclani Jotti, and M. Dowsett, “A ‘Quickscore’ Method for Immunohistochemical Semiquantitation: Validation for Oestrogen Receptor in Breast Carcinomas,” *Journal of Clinical Pathology* 48, no. 9 (1995): 876–878, <https://doi.org/10.1136/JCP.48.9.876>.
16. M. M. Mukaka, “Statistics Corner: A Guide to Appropriate Use of Correlation Coefficient in Medical Research,” *Malawi Medical Journal: The Journal of Medical Association of Malawi* 24, no. 3 (2012): 69–71.
17. F. E. Marginean, R. Hellsten, A. Krzyzanowska, and A. Bjartell, “Nuclear Expression of pSTAT3Tyr705 and pSTAT3Ser727 in the Stromal Compartment of Localized Hormone-Naïve Prostate Cancer,” *Pathology - Research and Practice* 232 (2022): 153811, <https://doi.org/10.1016/J.PRP.2022.153811>.
18. R. Cocchiola, E. Rubini, F. Altieri, et al., “STAT3 Post-Translational Modifications Drive Cellular Signaling Pathways in Prostate Cancer Cells,” *International Journal of Molecular Sciences* 20, no. 8 (2019): 1815, <https://doi.org/10.3390/IJMS20081815>.
19. J. Bishop, D. Thaper, and A. Zoubeidi, “The Multifaceted Roles of STAT3 Signaling in the Progression of Prostate Cancer,” *Cancers* 6, no. 2 (2014): 829–859, <https://doi.org/10.3390/CANCERS6020829>.
20. M. Sadrkhanloo, M. D. A. Paskeh, M. Hashemi, et al., “STAT3 Signaling in Prostate Cancer Progression and Therapy Resistance: An Oncogenic Pathway With Diverse Functions,” *Biomedicine & Pharmacotherapy = Biomedecine & Pharmacotherapie* 158 (2023): 114168, <https://doi.org/10.1016/J.BIOPHA.2022.114168>.
21. Y. Hua, W. Azeem, Y. Shen, et al., “Dual Androgen Receptor (Ar) and STAT3 Inhibition By a Compound Targeting the Ar Amino-Terminal Domain,” *Pharmacology Research & Perspectives* 6, no. 6 (2018), <https://doi.org/10.1002/PRP2.437>.
22. F. N. Hsu, M. C. Chen, K. C. Lin, et al., “Cyclin-Dependent Kinase 5 Modulates STAT3 and Androgen Receptor Activation Through Phosphorylation of Ser⁷²⁷ on STAT3 in Prostate Cancer Cells,” *American Journal of Physiology-Endocrinology and Metabolism* 305, no. 8 (2013): E975–E986, <https://doi.org/10.1152/AJPENDO.00615.2012>.
23. T. Ueda, N. Bruchovsky, and M. D. Sadar, “Activation of the Androgen Receptor N-Terminal Domain By Interleukin-6 Via Mapk and STAT3 Signal Transduction Pathways,” *Journal of Biological Chemistry* 277, no. 9 (2002): 7076–7085, <https://doi.org/10.1074/JBC.M108255200>.
24. D. S. Aaronson, M. Muller, S. R. Neves, et al., “An Androgen-IL-6-Stat3 Autocrine Loop Re-Routes EGF Signal in Prostate Cancer Cells,” *Molecular and Cellular Endocrinology* 270, no. 1–2 (2007): 50–56, <https://doi.org/10.1016/J.MCE.2007.02.006>.
25. E. Choi, J. Buie, J. Camacho, P. Sharma, and W. T. W. de Riese, “Evolution of Androgen Deprivation Therapy (ADT) and Its New Emerging Modalities in Prostate Cancer: An Update for Practicing Urologists, Clinicians and Medical Providers,” *Research and Reports in Urology* 14 (2022): 87–108, <https://doi.org/10.2147/RRU.S303215>.
26. P. P. Banerjee, S. Banerjee, T. R. Brown, and B. R. Zirkin, “Androgen Action in Prostate Function and Disease,” *American Journal of Clinical and Experimental Urology* 6, no. 2 (2018): 62–77.
27. J. J. Alumkal, D. Sun, E. Lu, et al., “Transcriptional Profiling Identifies an Androgen Receptor Activity-Low, Stemness Program Associated With Enzalutamide Resistance,” *Proceedings of the National Academy of Sciences* 117, no. 22 (2020): 12315–12323, https://doi.org/10.1073/PNAS.1922207117/SUPPL_FILE/PNAS.1922207117.SD01.XLSX.
28. Y. Wang, J. Chen, Z. Wu, et al., “Mechanisms of Enzalutamide Resistance in Castration-Resistant Prostate Cancer and Therapeutic Strategies to Overcome It,” *British Journal of Pharmacology* 178, no. 2 (2021): 239–261, <https://doi.org/10.1111/BPH.15300>.
29. D. E. Drachenberg, A. A. A. Elgamal, R. Rowbotham, M. Peterson, and G. P. Murphy, “Circulating Levels of Interleukin-6 in Patients With Hormone Refractory Prostate Cancer,” *The Prostate* 41 (1999): 127–133, [https://doi.org/10.1002/\(SICI\)1097-0045\(19991001\)41:2](https://doi.org/10.1002/(SICI)1097-0045(19991001)41:2).
30. A. Azevedo, “IL-6/IL-6R as a Potential Key Signaling Pathway in Prostate Cancer Development,” *World Journal of Clinical Oncology* 2, no. 12 (2011): 384, <https://doi.org/10.5306/WJCO.V2.I12.384>.
31. F. Handle, M. Pühr, G. Schaefer, et al., “The STAT3 Inhibitor Galiellalactone Reduces IL6-Mediated Ar Activity in Benign and Malignant Prostate Models,” *Molecular Cancer Therapeutics* 17, no. 12 (2018): 2722–2731, <https://doi.org/10.1158/1535-7163.MCT-18-0508>.
32. R. Hellsten, A. Stiehm, M. Palominos, M. Persson, and A. Bjartell, “The STAT3 Inhibitor GPB730 Enhances the Sensitivity to Enzalutamide in Prostate Cancer Cells,” *Translational Oncology* 24 (2022): 101495, <https://doi.org/10.1016/J.TRANON.2022.101495>.
33. D. Thaper, S. Vahid, R. Kaur, et al., “Galiellalactone Inhibits the STAT3/AR Signaling Axis and Suppresses Enzalutamide-Resistant Prostate Cancer,” *Scientific Reports* 8, no. 1 (2018): 17307, <https://doi.org/10.1038/S41598-018-35612-Z>.
34. C. Liu, Y. Zhu, W. Lou, Y. Cui, C. P. Evans, and A. C. Gao, “Inhibition of Constitutively Active Stat3 Reverses Enzalutamide Resistance in Lncap Derivative Prostate Cancer Cells,” *The Prostate* 74, no. 2 (2014): 201–209, <https://doi.org/10.1002/PROS.22741>.
35. C. Rébé and F. Ghiringhelli, “STAT3, a Master Regulator of Anti-Tumor Immune Response,” *Cancers* 11, no. 9 (2019): 1280, <https://doi.org/10.3390/CANCERS11091280>.
36. T. Wang, G. Niu, M. Kortylewski, et al., “Regulation of the Innate and Adaptive Immune Responses By Stat-3 Signaling in Tumor Cells,” *Nature Medicine* 10, no. 1 (2004): 48–54, <https://doi.org/10.1038/NM976>.
37. Z. Guo, H. Zhang, Y. Fu, et al., “Cancer-Associated Fibroblasts Induce Growth and Radioresistance of Breast Cancer Cells Through Paracrine Il-6,” *Cell Death Discovery* 9, no. 1 (2023): 6, <https://doi.org/10.1038/s41420-023-01306-3>.
38. A. Tsuyada, A. Chow, J. Wu, et al., “CCL2 Mediates Cross-Talk Between Cancer Cells and Stromal Fibroblasts That Regulates Breast Cancer Stem Cells,” *Cancer Research* 72, no. 11 (2012): 2768–2779, <https://doi.org/10.1158/0008-5472.CAN-11-3567>.
39. X. Li, Q. Xu, Y. Wu, et al., “A CCL2/ROS Autoregulation Loop Is Critical for Cancer-Associated Fibroblasts-Enhanced Tumor Growth of Oral Squamous Cell Carcinoma,” *Carcinogenesis* 35, no. 6 (2014): 1362–1370, <https://doi.org/10.1093/CARCIN/BGU046>.

40. A. Allam, M. Yakou, L. Pang, M. Ernst, and J. Huynh, "Exploiting the STAT3 Nexus in Cancer-Associated Fibroblasts to Improve Cancer Therapy," *Frontiers in Immunology* 12 (2021): 767939, <https://doi.org/10.3389/FIMMU.2021.767939/BIBTEX>.
41. J. Pan, Z. Ma, B. Liu, et al., "Identification of Cancer-Associated Fibroblasts Subtypes in Prostate Cancer," *Frontiers in Immunology* 14 (2023): 1133160, <https://doi.org/10.3389/FIMMU.2023.1133160/BIBTEX>.
42. D. Yang, J. Liu, H. Qian, and Q. Zhuang, "Cancer-Associated Fibroblasts: From Basic Science to Anticancer Therapy," *Experimental & Molecular Medicine* 55, no. 7 (2023): 1322–1332, <https://doi.org/10.1038/S12276-023-01013-0>.
43. H. Wang, N. Li, Q. Liu, et al., "Antiandrogen Treatment Induces Stromal Cell Reprogramming to Promote Castration Resistance in Prostate Cancer," *Cancer Cell* 41, no. 7 (2023): 1345–1362.e9, <https://doi.org/10.1016/J.CCELL.2023.05.016>.
44. K. S. Chun, J. H. Jang, and D. H. Kim, "Perspectives Regarding the Intersections Between STAT3 and Oxidative Metabolism in Cancer," *Cells* 9, no. 10 (2020): 2202, <https://doi.org/10.3390/CELLS9102202>.
45. J. Arévalo, D. Lorente, E. Trilla, M. T. Salcedo, J. Morote, and A. Meseguer, "Nuclear and Cytosolic pS727-STAT3 Levels Correlate With Overall Survival of Patients Affected By Clear Cell Renal Cell Carcinoma (Ccrcc)," *Scientific Reports* 11, no. 1 (2021): 6957, <https://doi.org/10.1038/S41598-021-86218-X>.
46. E. Morrow, K. Pennel, P. Hatthakarnkul, et al., "High Expression of STAT3 Within the Tumour-Associated Stroma Predicts Poor Outcome in Breast Cancer Patients," *Cancer Medicine* 12, no. 12 (2023): 13225–13240, <https://doi.org/10.1002/CAM4.6014>.

Supporting Information

Additional supporting information can be found online in the Supporting Information section.